Smooth spline wavelets on the sphere

Jan Maes and Adhemar Bultheel

Abstract. The lifting scheme provides an easy way to construct wavelet bases on manifolds of arbitrary topological type. In this paper we use a standard two-step lifted wavelet transform to construct spherical Powell–Sabin (PS) spline wavelets. The first lifting step or prediction step consists of a PS spline subdivision scheme that is based on $\sqrt{3}$ refinement of the underlying spherical triangulation. The second lifting step or update step is used to achieve certain properties for the wavelets such as a vanishing moment and approximate semi-orthogonality.

§1. Spherical Powell–Sabin splines

In a series of papers [1, 2, 3], Alfeld *et al.* develop spline spaces on triangulations on the sphere analogous to the classical spline spaces on planar triangulations. The idea is to work with homogeneous Bernstein–Bézier polynomials in $\mathbb{R}^3$ which are then restricted to the sphere. A function f defined on $\mathbb{R}^3$ is homogeneous of degree d provided that $f(\alpha v) = \alpha^d f(v)$ for all real α and all $v \in \mathbb{R}^3$. The space $\mathbb{H}_d$ of trivariate polynomials of degree d that are homogeneous of degree d is a $\binom{d+2}{2}$ dimensional subspace of the space of trivariate polymials of degree d. If we restrict $\mathbb{H}_d$ to any hyperplane H in $\mathbb{R}^3 \setminus \{0\}$, then we just recover the well-known space of bivariate polynomials on H. Similarly, let Ω be any subset of the unit sphere S, then we define $\mathbb{H}_d(\Omega)$ as the restriction of $\mathbb{H}_d$ to Ω and we refer to it as the space of spherical polynomials of degree d on Ω. Let Δ be a conforming spherical triangulation of $\Omega \subseteq S$, cfr. [12]. Then we define the space of spherical splines of degree d and smoothness r associated with Δ as

$$S_d^r(\Delta) := \{s \in C^r(S) \mid s|_\tau \in \mathbb{H}_d(\tau),\ \tau \in \Delta\},$$

where $s|_\tau$ denotes the restriction of s to the spherical triangle τ.

In general, maintaining C^1 continuity conditions between neighbouring triangles results in non-trivial relations, see, e.g., [6]. Therefore, to

Conference Title
Editors pp. 1–6.
Copyright © 2005 by Nashboro Press, Brentwood, TN.
ISBN 0-0-9728482-x-x
All rights of reproduction in any form reserved.

overcome this problem, we will focus on the Powell–Sabin 6-split of a triangulation. Starting from an arbitrary spherical triangulation Δ, we introduce further substructures by subdividing each triangle of Δ into 6 subtriangles as shown schematically in Fig. 1. We will refer to this new triangulation as Δ^{PS}. The spline space $S_2^1(\Delta^{PS})$ of piecewise quadratic C^1 spherical polynomials over Δ^{PS} will be called the space of spherical Powell–Sabin splines. Let g_i and h_i be independent unit vectors lying in the tangent plane of S at the vertices v_i, $i = 1, \ldots, n$, of Δ. A spline function $s \in S_2^1(\Delta^{PS})$ will be uniquely defined by the following interpolation problem. Given any set of values $(\alpha_i, \beta_i, \gamma_i)$, $i = 1, \ldots, n$, there is a unique $s(v) \in S_2^1(\Delta^{PS})$ such that

$$s(v_i) = \alpha_i, \quad D_{g_i} s(v_i) = \beta_i, \quad D_{h_i} s(v_i) = \gamma_i, \tag{1}$$

for all $i = 1, \ldots, n$. Hence, $S_2^1(\Delta^{PS})$ has dimension $3n$ with n the number of vertices in Δ. We refer to [10] for all the details.

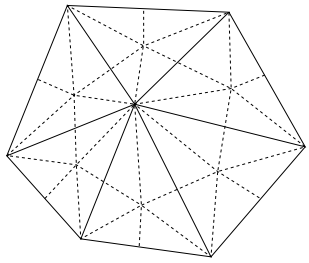

Fig. 1. Schematic representation of a PS 6-split of a triangulation Δ.

§2. B-spline representation for the space $S_2^1(\Delta^{PS})$

If for each vertex v_i in Δ we choose numbers $(\alpha_{ij}, \beta_{ij}, \gamma_{ij})$, $j = 1, 2, 3$, that form a set of 3 linear independent triplets, then every $s(v) \in S_2^1(\Delta^{PS})$ has a unique representation

$$s(v) = \sum_{i=1}^{n} \sum_{j=1}^{3} c_{ij} B_{ij}(v) \tag{2}$$

where the splines $B_{ij}(v)$ are defined as the solution of the interpolation problem (1) with

$$(\alpha_k, \beta_k, \gamma_k) = (\delta_{ik}\alpha_{ij}, \delta_{ik}\beta_{ij}, \delta_{ik}\gamma_{ij}), \qquad k = 1, \ldots, n,$$

where δ_{ik} represents the Kronecker delta. Such a spline $B_{ij}(v)$ has local support and will further be called a spherical PS B-spline.

In [11] we give an algorithm to compute suitable triplets $(\alpha_{ij}, \beta_{ij}, \gamma_{ij})$, $j = 1, 2, 3$, such that the corresponding B-splines form a convex partition of unity on Ω, i.e.,

$$B_{ij}(v) \geq 0 \text{ for all } v \in \Omega$$

$$\sum_{i=1}^{n} \sum_{j=1}^{3} B_{ij}(v) = 1 \text{ for all } v \in \Omega.$$

These B-splines are a spherical extension of the bivariate B-spline basis developed by Dierckx in [5].

There is a nice geometric interpretation that can be given to these B-splines. For each vertex v_i in Δ we can define a (planar) PS-triangle $t_i(Q_{i1}, Q_{i2}, Q_{i3})$ that is tangent to the unit sphere S at v_i. This PS-triangle has to satisfy some simple conditions, see [11]. Next we define three control points

$$C_{ij} := Q_{ij} + c_{ij} v_i, \quad j = 1, 2, 3.$$

Orthogonal projection of C_{ij} on the tangent plane to S at v_i gives Q_{ij}, and the distance between Q_{ij} and C_{ij} is given by $|c_{ij}|$. These control points C_{ij} constitute control triangles $\mathscr{T}_i(C_{i1}, C_{i2}, C_{i3})$. One can prove ([11]) that the control triangle $\mathscr{T}_i$ is tangent to the surface $(s(v) + 1)v$, $v \in S$, at vertex v_i, see Fig. 2.

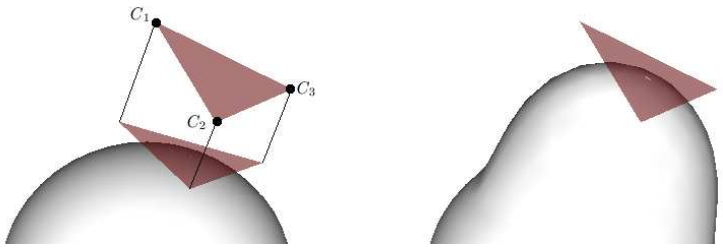

(a) PS-triangle and control triangle (b) Corresponding PS spline surface

Fig. 2. Control triangles as tools for modeling the shape of the spline surface. (a) The triangle tangent to the sphere is the PS-triangle. The control triangle is defined by the three control points C_1, C_2, C_3. The orthogonal projection of the three control points onto the plane defined by the PS-triangle coincides with the vertices of the PS-triangle. (b) The resulting Powell–Sabin spline surface is tangent to the control triangle.

§3. Spline subdivision

The goal of spline subdivision is to compute the B-spline representation (2) of a PS spline surface on a refinement of a given triangulation. In

order to create nested spherical PS spline spaces

$$S_2^1(\Delta_0^{PS}) \subset S_2^1(\Delta_1^{PS}) \subset S_2^1(\Delta_2^{PS}) \subset \cdots \tag{3}$$

it is sufficient that we find a refinement procedure that yields nested sequences

$$\Delta_0^{PS} \subset \Delta_1^{PS} \subset \Delta_2^{PS} \subset \cdots ,$$
$$\{v_i \in \Delta_0\} \subset \{v_i \in \Delta_1\} \subset \{v_i \in \Delta_2\} \subset \cdots .$$

It was pointed out by Vanraes *et al.* [15] that applying a $\sqrt{3}$ refinement scheme yields nested PS spline spaces. Applying the $\sqrt{3}$ scheme twice yields a triadic scheme. The $\sqrt{3}$ scheme was first introduced by Kobbelt [7] and Labsik and Greiner [8]. Instead of splitting each edge in Δ_0 and performing a 1-to-4 split for each triangle (dyadic refinement), we compute a new vertex for each triangle and retriangulate the old and new vertices. Fig. 3 shows the principle. Note that the new edges in Δ_1 coincide with the lines of the PS 6-split Δ_0^{PS}, and that for any triangle in Δ_1 there exists exactly one edge in Δ_0 that crosses this triangle. In the new triangles new interior points must be chosen on this unique edge from Δ_0 that crosses the triangle.

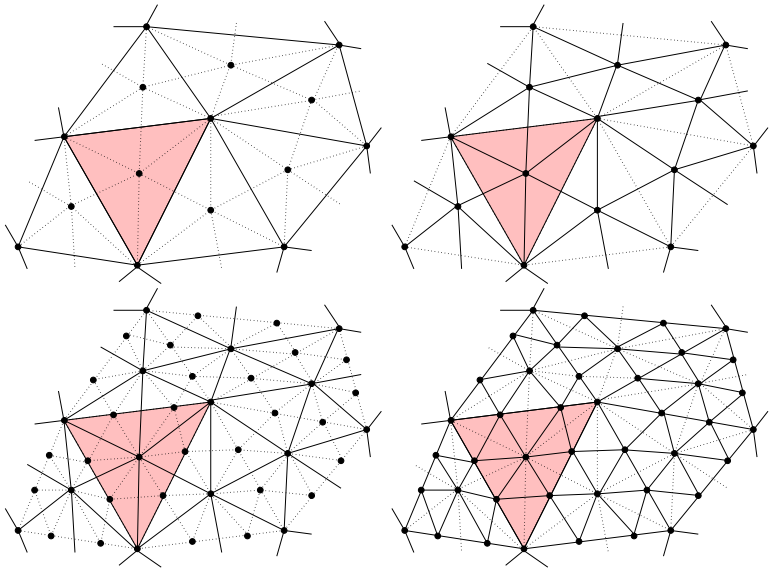

Fig. 3. Principle of $\sqrt{3}$ subdivision. Applying the $\sqrt{3}$ subdivision twice results in triadic subdivision.

It will be convenient to use matrix notation. Denote by Φ^j the column vector that contains all the PS B-splines that span the PS spline space

$S^j := S_2^1(\Delta_j^{PS})$, with j the resolution level. From now on we will refer to the elements of Φ^j as scaling functions. Because of (3) the scaling functions satisfy a refinement equation of the form

$$\Phi^j = \mathbf{P}^j \Phi^{j+1}, \tag{4}$$

where $\mathbf{P}^j$ is called the subdivision matrix.

§4. Multiscale decomposition via lifting

The space S^{j+1} describes more detail of a surface than the coarser space S^j. The difference can be captured in a complementary space W^j such that

$$S^j \oplus W^j = S^{j+1}.$$

The complement space W^j is not necessarily orthogonal to S^j. We will refer to the basis functions of W^j as wavelets and we collect them in a column vector Ψ^j. In analogy with (4), the relation between Ψ^j and Φ^{j+1} is given by a filter $\mathbf{Q}^j$

$$\Psi^j = \mathbf{Q}^j \Phi^{j+1}.$$

Every function in S^{j+1} can be written as a low resolution part in S^j and a detail part in W^j

$$\mathbf{s}^{j+1}\Phi^{j+1} = \mathbf{s}^j \Phi^j + \mathbf{w}^j \Psi^j,$$

where $\mathbf{s}^j$ and $\mathbf{w}^j$ are row vectors that contain the coefficients. This is done with two analysis filters, a low pass filter $\mathbf{A}^j$ and a high pass filter $\mathbf{B}^j$

$$\begin{aligned} \mathbf{s}^j &= \mathbf{s}^{j+1}\mathbf{A}^j \\ \mathbf{w}^j &= \mathbf{s}^{j+1}\mathbf{B}^j. \end{aligned}$$

Since

$$\begin{bmatrix} \Phi^j \\ \Psi^j \end{bmatrix} = \begin{bmatrix} \mathbf{P}^j \\ \mathbf{Q}^j \end{bmatrix} \Phi^{j+1}$$

one can easily see that the analysis filters must be defined by the inverse relation

$$\begin{bmatrix} \mathbf{A}^j & \mathbf{B}^j \end{bmatrix}^{-1} = \begin{bmatrix} \mathbf{P}^j \\ \mathbf{Q}^j \end{bmatrix}$$

and $\mathbf{s}^{j+1}$ can be recovered from $\mathbf{s}^j$ and $\mathbf{w}^j$ using the synthesis filters $\mathbf{P}^j$ and $\mathbf{Q}^j$

$$\mathbf{s}^{j+1} = \mathbf{s}^j \mathbf{P}^j + \mathbf{w}^j \mathbf{Q}^j.$$

The subdivision matrix $\mathbf{P}^j$ can be written in block matrix form as

$$\mathbf{P}^j = \begin{bmatrix} \mathbf{O}^j & \mathbf{N}^j \end{bmatrix}$$

where we distinguish a part $\mathbf{O}^j$ that computes the coefficients that are associated with the old vertices of Δ_j on the finer domain Δ_{j+1}, and a part $\mathbf{N}^j$ that computes the coefficients that are associated with the newly introduced vertices in Δ_{j+1}. Similarly we split Φ^{j+1} in functions $\mathcal{O}^{j+1}$ associated with the old vertices in Δ_{j+1} and functions $\mathcal{N}^{j+1}$ associated with the new vertices added when going from Δ_j to Δ_{j+1}

$$\Phi^{j+1} = \begin{bmatrix} \mathcal{O}^{j+1} \\ \mathcal{N}^{j+1} \end{bmatrix}.$$

The sets Φ^j and $\mathcal{N}^{j+1}$ together span S^{j+1} because the matrix $\mathbf{O}^j$ is invertible. Obviously the functions in $\mathcal{N}^{j+1}$ can be used as wavelet functions

$$\Psi^j = \mathcal{N}^{j+1} \quad \text{and} \quad \mathbf{Q}^j = \begin{bmatrix} \mathbf{0} & \mathbf{I} \end{bmatrix}.$$

Here $\mathbf{0}$ stands for the zero matrix and $\mathbf{I}$ stands for the identity matrix. By choosing the wavelet functions as the scaling functions on the finer level, we also made a choice for the complement space W^j. It can be desirable to have another complement space with certain properties. The wavelet functions can be found by projecting the $\mathcal{N}^{j+1}$ into the desired complement space W^j along S^j

$$\Psi^j = \mathcal{N}^{j+1} - \boldsymbol{\alpha}^j \Phi^j.$$

This projection is not necessarily orthogonal. For each wavelet function there is a corresponding row in $\boldsymbol{\alpha}^j$. The possibly nonzero entries in this row together will be called the stencil for that wavelet function. Note that if there are no zero entries in $\boldsymbol{\alpha}^j$, the wavelets will have the whole domain Ω as their support.

The reconstruction or synthesis filter in block matrix form is now

$$\begin{bmatrix} \mathbf{P}^j \\ \mathbf{Q}^j \end{bmatrix} = \begin{bmatrix} \mathbf{O}^j & \mathbf{N}^j \\ -\boldsymbol{\alpha}^j \mathbf{O}^j & \mathbf{I} - \boldsymbol{\alpha}^j \mathbf{N}^j \end{bmatrix}.$$

Because $\mathbf{O}^j$ is invertible, the filterbank operation is also easily invertible and we find the analysis filters $\mathbf{A}^j$ and $\mathbf{B}^j$

$$\begin{bmatrix} \mathbf{A}^j & \mathbf{B}^j \end{bmatrix} = \begin{bmatrix} (\mathbf{O}^j)^{-1} - (\mathbf{O}^j)^{-1}\mathbf{N}^j\boldsymbol{\alpha}^j & -(\mathbf{O}^j)^{-1}\mathbf{N}^j \\ \boldsymbol{\alpha}^j & \mathbf{I} \end{bmatrix}.$$

These filters can be factored as follows

$$\begin{bmatrix} \mathbf{P}^j \\ \mathbf{Q}^j \end{bmatrix} = \begin{bmatrix} \mathbf{I} & \mathbf{0} \\ -\boldsymbol{\alpha}^j & \mathbf{I} \end{bmatrix} \cdot \begin{bmatrix} \mathbf{I} & \mathbf{N}^j \\ \mathbf{0} & \mathbf{I} \end{bmatrix} \cdot \begin{bmatrix} \mathbf{O}^j & \mathbf{0} \\ \mathbf{0} & \mathbf{I} \end{bmatrix}$$

and

$$\begin{bmatrix} \mathbf{A}^j & \mathbf{B}^j \end{bmatrix} = \begin{bmatrix} (\mathbf{O}^j)^{-1} & \mathbf{0} \\ \mathbf{0} & \mathbf{I} \end{bmatrix} \cdot \begin{bmatrix} \mathbf{I} & -\mathbf{N}^j \\ \mathbf{0} & \mathbf{I} \end{bmatrix} \cdot \begin{bmatrix} \mathbf{I} & \mathbf{0} \\ \boldsymbol{\alpha}^j & \mathbf{I} \end{bmatrix}.$$

This relates to the concept of lifting [14]. Every factor in the factorization of the filters corresponds to a lifting step. The filter bank factored in lifting steps is shown in Fig. 4.

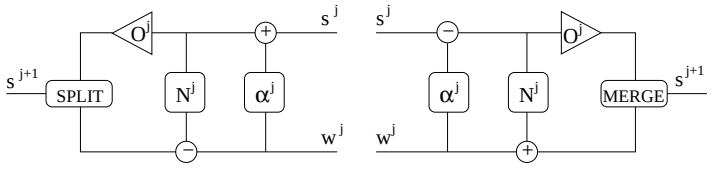

Fig. 4. Filter bank factored in lifting steps.

First the coefficients $\mathbf{s}^{j+1}$ are split into two sequences. The first sequence, $\mathbf{s}_o^{j+1}$, contains the coefficients that correspond to vertices in Δ_j, and the second sequence, $\mathbf{s}_n^{j+1}$, contains coefficients that correspond to vertices that are in Δ_{j+1} but not in Δ_j. The subscripts o and n refer to old and new vertices during the subdivision process.

Then we want to treat $\mathbf{s}_o^{j+1}$ as the coefficients of a surface defined on Δ_j. Therefore we first need to scale the coefficients of the old vertices with $\mathbf{O}^{j^{-1}}$. After this we can apply the part $\mathbf{N}^j$ of the subdivision algorithm $\mathbf{P}^j$ that leads to the coefficients for the new vertices. The result is used as a prediction for $\mathbf{s}_n^{j+1}$ and substracted from this sequence. This yields the wavelet coefficients $\mathbf{w}^j$ on the lower branch in the picture. We call this step the prediction step. Finally $\mathbf{s}_o^{j+1}$ is updated with a linear combination defined by $\boldsymbol{\alpha}^j$ of wavelet coefficients $\mathbf{w}^j$. This yields the scaling coefficients $\mathbf{s}^j$ on the upper branch in the picture. We call this step the update step.

Reversing the lifting scheme is straightforward: we run through the scheme backwards, replace plus with minus signs, undo scaling operations and merge what had been split. So unlike the classical wavelet transform where $\mathbf{A}^j$, $\mathbf{B}^j$, $\mathbf{P}^j$ and $\mathbf{Q}^j$ are used explicitly, the same filters $\mathbf{O}^j$, $\mathbf{N}^j$ and $\boldsymbol{\alpha}^j$ appear now in the forward and inverse transform.

§5. Design of the update step

Without an update step the multilevel system $\boldsymbol{\Psi} := \Phi^0 \cup \bigcup_{j=0}^{\infty} \Psi^j$ consists of scaling functions on several resolution levels. More particular we have $\boldsymbol{\Psi} = \Phi^0 \cup \bigcup_{j=0}^{\infty} \mathcal{N}^j$ which is just the standard hierarchical basis. It is well known that standard hierarchical bases do not form Riesz bases for L_2. For instance they do not have a vanishing moment which is required, [4]. We use the update to achieve properties that the unlifted wavelets do not have.

There is a simple update method that is provably stable. One can choose the update operator $\boldsymbol{\alpha}^j$ as the L_2-orthogonal projection from S^{j+1}

onto S^j. This yields a multiscale decomposition in which the complement spaces W^j are L_2-orthogonal complements to S^j in S^{j+1}. The resulting multilevel system $\mathbf{\Psi}$ is a Riesz basis for L_2 and the wavelets are orthogonal to all polynomials in S^0. Unfortunately, in general the matrix $\boldsymbol{\alpha}^j$ is full, so that the lifted wavelets are not locally supported but stretch out over the whole domain Ω. This is a major disadvantage for many applications. The update matrix $\boldsymbol{\alpha}^j$ has however an interesting property in this case. Even when $\boldsymbol{\alpha}^j$ is full it has an exponential off-diagonal decay of a rate that is independent of j, see [13] for a proof. Hence the idea of approximating $\boldsymbol{\alpha}^j$ by a truncated matrix [9, 13, 16]. Because of the off-diagonal decay, truncating $\boldsymbol{\alpha}^j$ yields a banded matrix. Local semi-orthogonalization exploits this property. One fixes the stencil and the scaling functions that come in the update step in advance and then one orthogonalizes each wavelet function to the subset of S^j that is defined by the stencil. The lifted wavelets will be approximately orthogonal to S^j. To enforce a vanishing moment one can add a linear constraint that forces each wavelet to have a vanishing moment, and the other degrees of freedom make the wavelet as orthogonal as possible in a least squares sense to its predefined set of scaling functions.

In our construction we have chosen to update the three wavelet functions that are associated with a newly introduced vertex v in Δ_{j+1} by the nine scaling functions that are associated with the three surrounding old vertices in Δ_j that constitute the triangle in Δ_j that contains v as an interior point. Fig. 5 shows the three wavelet functions.

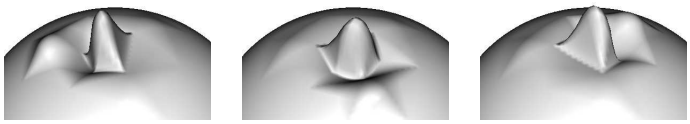

Fig. 5. The three spherical PS spline wavelets that are associated with a vertex.

§6. Applications

Wavelets have been used in a broad range of applications such as data compression, computer graphics and numerical analysis. In this section the spherical PS spline wavelets are applied to some graphics problems, see Fig. 6. The spherical PS spline surface in Fig. 6 (a) is obtained by approximating laser range data, originally provided through the courtesy of Cyberware, in a least squares sense. The underlying triangulation Δ_6 is constructed from a regular icosahedron projected onto the sphere which was then subdivided six times.

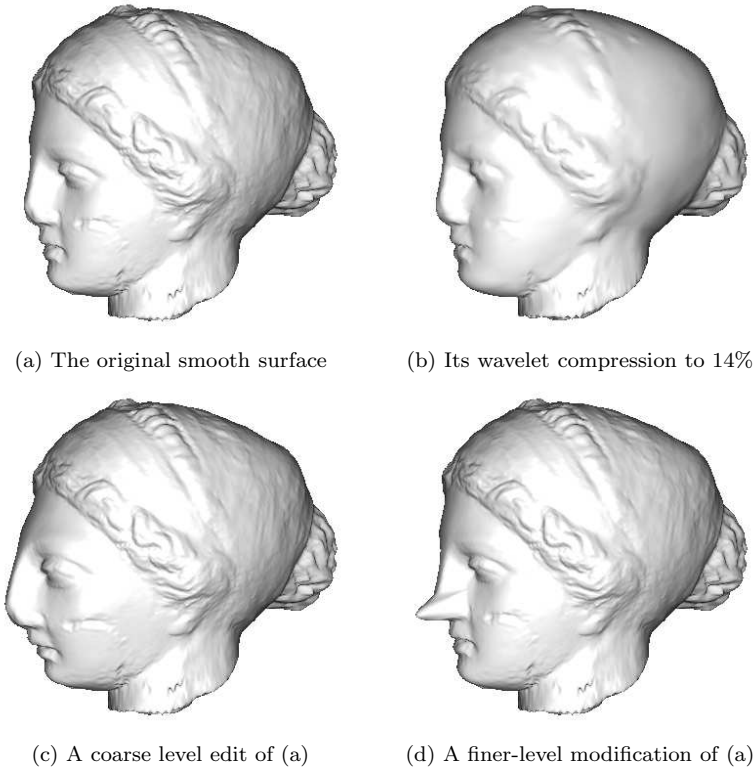

(a) The original smooth surface (b) Its wavelet compression to 14%

(c) A coarse level edit of (a) (d) A finer-level modification of (a)

Fig. 6. Compression and multiresolution editing of a smooth surface.

References

1. P. Alfeld, M. Neamtu, and L. L. Schumaker. Bernstein–Bézier polynomials on spheres and sphere-like surfaces. Comput. Aided Geom. Design, **13**(4):333–349, 1996.
2. P. Alfeld, M. Neamtu, and L. L. Schumaker. Dimension and local bases of homogeneous spline spaces. SIAM J. Math. Anal., **27**(5):1482–1501, 1996.
3. P. Alfeld, M. Neamtu, and L. L. Schumaker. Fitting scattered data on sphere-like surfaces using spherical splines. J. Comput. Appl. Math., **73**(1-2):5–43, 1996.
4. W. Dahmen. Some remarks on multiscale transformations, stability and biorthogonality. In P. J. Laurent, A. Le Méhauté, and L. L. Schumaker, editors, *Curves and surfaces*. Academic Press, 1994.

5. P. Dierckx. On calculating normalized Powell–Sabin B-splines. Comput. Aided Geom. Design, **15**(1):61–78, 1997.
6. G. Farin. *Curves And Surfaces For Computer Aided Geometric Design: A Practical Guide*. Academic Press, Boston, 4th edition, 1997.
7. L. Kobbelt. $\sqrt{3}$-subdivision. In *Computer Graphics Proceedings*, Annual Conference Series, pages 103–112. ACM SIGGRAPH, 2000.
8. U. Labsik and G. Greiner. Interpolatory $\sqrt{3}$-subdivision. Comput. Graph. Forum, **19**(3):131–138, 2000.
9. M. Lounsbery, T. D. DeRose, and J. Warren. Multiresolution analysis for surfaces of arbitrary topological type. ACM Trans. on Graphics, **16**(1):34–73, 1997.
10. J. Maes and A. Bultheel. A hierarchical basis preconditioner for the biharmonic equation on the sphere. IMA J. Numer. Anal., **26**(3):563–583, 2006.
11. J. Maes and A. Bultheel. Modeling genus zero closed manifolds with spherical Powell–Sabin B-splines. 2006. Submitted.
12. L. L. Schumaker. Triangulations in CAGD. IEEE Comp. Graph. Appl., **13**:47–52, 1993.
13. J. Simoens and S. Vandewalle. A stabilized lifting construction of wavelets on irregular meshes on the interval. SIAM J. Scient. Computing, **24**(4):1356–1378, 2002.
14. W. Sweldens. The lifting scheme: A construction of second generation wavelets. SIAM J. Math. Anal., **29**(2):511–546, 1997.
15. E. Vanraes, J. Windmolders, A. Bultheel, and P. Dierckx. Automatic construction of control triangles for subdivided Powell–Sabin splines. Comput. Aided Geom. Design, **21**(7):671–682, 2004.
16. P. S. Vassilevski and J. Wang. Stabilizing the hierarchical basis by approximate wavelets I: Theory. Num. Lin. Alg. Appl., **4**(2):103–126, 1997.

Jan Maes
Dept. of Computer Science, Katholieke Universiteit Leuven
Celestijnenlaan 200A, B-3001 Heverlee, Belgium
`jan.maes@cs.kuleuven.be`

This work is partially supported by the Flemish Fund for Scientific Research (FWO Vlaanderen) projects MISS (G.0211.02) and SMID (G.0431.05), and by the Belgian Programme on Interuniversity Attraction Poles, initiated by the Belgian Federal Science Policy Office. The scientific responsibility rests with the authors.